
First Principles Study of CO Adsorption on Atomic Pd Supported on Metal Oxide Surfaces (ZrO₂(110), MgO(100), CeO₂(110))

Tetsuya Ohkawa^{*}, Kei Kuramoto

Department of Electrical Engineering and Computer Sciences, University of Hyogo, Himeji, Hyogo, Japan

Email address:

univhyogoohkawat@gmail.com (T. Ohkawa)

^{*}Corresponding author

To cite this article:

Tetsuya Ohkawa, Kei Kuramoto. First Principles Study of CO Adsorption on Atomic Pd Supported on Metal Oxide Surfaces (ZrO₂(110), MgO(100), CeO₂(110)). *International Journal of Computational and Theoretical Chemistry*. Vol. 4, No. 3, 2016, pp. 31-40.

doi: 10.11648/j.ijctc.20160403.13

Received: December 15, 2016; **Accepted:** December 30, 2016; **Published:** January 17, 2017

Abstract: We have performed density functional theory (DFT) quantum periodic calculations to investigate the interaction between atomic Pd and oxide surfaces of ZrO₂(110), MgO(100), and CeO₂(110). In this calculation, Pd adsorption energy on the surface oxygen atom sites of those oxide surfaces correlated with the position of the d electron density center of Pd atom except for on the surface metal atom site. Furthermore, CO adsorption on Pd atoms adsorbed on the surface of those three kinds of oxide surfaces was investigated. The CO adsorption energy did not correlate with the position of d electron density center of Pd at the adsorption sites when they are summarized on each oxide surface but correlated with it when three kinds of oxide surface are grouped by adsorption site. Since Pd atom is the smallest size, it is easily influenced by oxide surface atoms and adsorbates. These results suggest that the nature of Pd atom adsorbed on oxide surface changes depending on where Pd atoms adsorb on the oxide surface, and is controlled by d electron density center.

Keywords: Pd-oxide Surface Interaction, CO Adsorption, d Electron Density Center, Density Functional Theory Calculation

1. Introduction

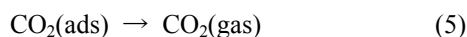
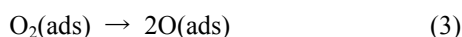
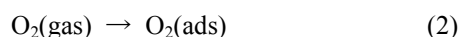
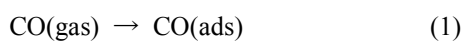
CO oxidation reaction on Pt-group metal surface such as Platinum (Pt), Palladium (Pd), and Rhodium (Rh) has been studied to understand the prototypical catalytic reaction on metal surface. For instance, this reaction is widely used in industrial applications such as three-way automotive catalyst. The ability of catalyst which accelerates the chemical reaction has been used widely.

Pt supported on ceria-zirconia (CeO₂-ZrO₂) solid solution is put to practical use as a three-way automotive catalyst purifying automobile exhaust gas. However, Pt is noble metal and high cost. Moreover, the adsorption of much amount of CO on Pt-group metal surface inhibit the dissociative reaction of O₂ because O₂ cannot adsorbed on the surface, which is so-called CO poisoning [1, 2]. Therefore, the alternative metal catalyst is important to reduce the cost and use of the scarce resources, and enhance the CO tolerance. Pd is one of the alternative resources because it is more

abundant and less expensive and has a higher CO tolerance than Pt, and it shows similar catalytic behaviour and durability in acidic media [3]. In addition, Pd exhibit a high reactivity for CO oxidation reaction, and this ability has led to their widespread use in automobile exhaust converter [4], and Pd supported on CeO₂ is an effective catalytic material for three-way automotive catalysis [5]. Furthermore, Pd alloy with other metals shows enhanced catalytic activity and CO tolerance in CO oxidation reaction [6-8]. For instance, Pd-Au alloy catalysts have been demonstrated to promote CO oxidation reaction even at room temperature [6]. Theoretical studies can provide fundamental information with atomic and molecular scale for understanding the chemical reaction including CO oxidation reaction. Ham *et al.* performed density functional theory - generalized gradient approximation (DFT-GGA) calculation to examine the adsorption and oxidation of CO molecules on AuPd(111) alloy surfaces [3]. They reported that small Pd ensembles such as dimers and compact trimers tend to provide more

active sites than larger ensembles; CO adsorbed on Pd monomer is found to react hardly with O₂ to form CO₂.

On the other hand, it is recently reported that nano size materials show great catalytic activity as compared to bulk size ones [9-16]. For examples, Au has attracted much attention in recent years since the high activity of Au nanoparticles was reported by Haruta *et al* [9]. When Au is highly dispersed on oxide support surface, it can exhibit surprisingly high catalytic activity. Au clusters with or without oxide support can function as good catalysts in a wide chemical reaction such as selective hydrogenations [17, 18], propylene epoxidation [19,20], water-gas shift [17, 21, 22], etc. Furthermore, improvements of C-H bond activation as well as methane (CH₄) adsorption on various surfaces such as ad-atom, terraces, and steps as compared to the perfect flat surfaces are reported by theoretical studies [23-26]. For instance, Yuan *et al.* studied the dehydrogenation processes of CH₄ on the flat Cu(100), Cu ad-atom on Cu(100) surface (Cu@Cu(100)), and Ni@Cu(100) surface via spin polarized density functional theory (DFT) approach, and their calculated results showed that the reaction barrier for methane dehydrogenation were remarkably reduced by about 40%-60% with the assistant of the adsorbed Ni atom on the Cu(100) surface [23]. Therefore, we focus on the catalytic ability of Pd catalyst for CO oxidation reaction with atomic and molecular level. The elementary reactions of CO oxidation reaction on catalytic surface are as follows:

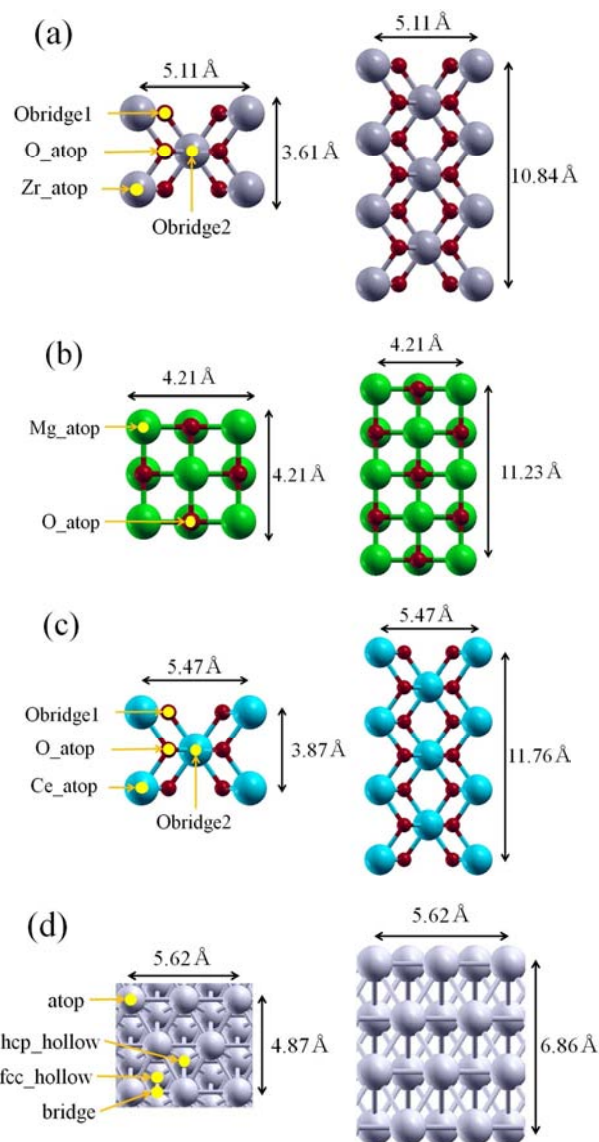


The reaction rate is limited by one elementary reaction out of the consecutive steps generally consist of adsorption, chemical reaction, and desorption [27, 28]. For CO oxidation reaction, the reaction rate is generally limited by the adsorption and dissociation reaction of O₂ molecule [29], but it is also necessary to trap CO molecule to promote CO oxidation reaction. The atomic Pd may become the good CO trap materials on an oxide surface because of the high reactivity of Pd for CO oxidation reaction. Moreover, it is important to understand the mechanism of catalytic reaction and behaviors of adsorbates on catalyst surface.

In this paper, we investigate the interaction between atomic Pd and oxide support surfaces of ZrO₂(110), CeO₂(110), and magnesia(100) (MgO) by comparing adsorption energies and electron density distribution of valence band of atomic Pd provided by DFT calculation, in particular for the adsorption of CO on these surface models. Moreover, we compared the calculated results mentioned the above with single Pd(111) crystal surface.

2. Computational Method

Reaction activity and electronic state of the adsorption atom on material surface are known to be controlled by electron density distribution of the valence band [30]. In this study, we pay attention to the interaction between Pd atom and material surface. In our study, the plane-wave method with the ultrasoft pseudo-potentials is adopted. We performed plane-wave periodic DFT calculation implemented with the Quantum Espresso package [31]. The Perdew-Wang (PW91) of GGA is used to incorporate exchange and correlation energies [32]. A plain wave basis set with a kinetic energy cutoff of 30 Ry is employed for the valence electrons. A fermi smearing of 0.01 Ry is utilized to determine electronic occupancies. A sampling of 4×4×1 k-points of the Monkhorst-Pack [33] scheme is used to model the Brillouin zone. Force less than 0.001 eV/Å is used as the criterion for the relaxation convergence. The relaxation of the electronic degrees of freedom is thought to be converged when the energy differences are less than 5×10⁻⁶ eV.



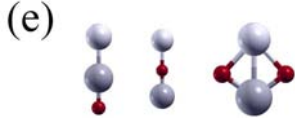


Figure 1. Metal oxide surfaces of (a) ZrO₂(110), (b) MgO(100), (c) CeO₂(110), (d) single Pd(111) crystal surface, and (e) simple atomic models (O-Zr-Pd, Zr-O-Pd, ZrOO-Pd as examples). Left and right side figures are the top and side view, respectively. Dark gray, green, blue, red, and white gray denote Zr, Mg, Ce, O, and Pd atoms, respectively. O-Zr-Pd, Zr-O-Pd, ZrOO-Pd represent the Pd bonding to Zr, oxygen, the center of two-oxygen atoms, respectively.

Figure 1 illustrates the oxide support surfaces, single Pd(111) crystal surface models, and simple atomic models, and also illustrates the adsorption sites for Pd on each oxide and Pd(111) surfaces. ZrO₂(110), MgO(100), CeO₂(110), and Pd(111) surfaces are modelled as 5.11×3.61×10.84, 4.21×4.21×11.23, 5.47×3.87×11.87, and 5.62×4.87×6.86 Å unit cell, respectively. A more than 10 Å vacuum slab is inserted into the direction perpendicular to the surface to separate the neighboring repeated slabs and ensure that the adsorbates and the repeated slab would not interact. In addition, simple molecular models were constructed to compare with oxide surface models.

Four types of adsorption site candidates are shown in Figure 1 with yellow circle, and adsorption energy of Pd atom on oxide surface is calculated from the following formula:

$$E = E_{Pd/M} - E_M - E_{Pd} \quad (6)$$

where E_{Pd} is the total energy of the Pd, E_M is the total energy of the M oxide supports (ZrO₂(110), MgO(100), CeO₂(110)), and $E_{Pd/M}$ is the total energy when Pd adsorbed on M oxide supports. After an adsorption site of the Pd was decided, we calculate adsorption energies of CO on Pd/M catalysts. The adsorption energies of CO are as follows:

$$E = E_{CO/Pd/M} - E_{Pd/M} - E_{CO} \quad (7)$$

where $E_{CO/Pd/M}$ is the total energy of CO adsorbed Pd/M catalyst and E_{CO} is the total energy of CO molecule.

3. Results and Discussion

3.1. Atomic Pd Adsorption on Oxide Surfaces

We first calculate the adsorption energy of Pd on ZrO₂(110), MgO(100), and CeO₂(110) oxide supports to evaluate where the adsorption sites of each oxide supports are the most stable site for Pd atom. Pd adsorption energies on each adsorption site of oxide supports are shown in Table 1. The most stable Pd adsorption site of ZrO₂ is O_{atop} site where Pd atom is positioned directly above a ZrO₂ surface oxygen atom and the calculated Pd adsorption energy is -2.356 eV, but Pd on Obridge1 site of ZrO₂ where Pd is positioned at the center between two surface oxygen atoms is slightly less stable than that on O_{atop} site (-2.287 eV). The most unstable Pd adsorption site is Zr_{atop} site where Pd is positioned directly above the surface Zr atom and the

calculated Pd adsorption energy is -1.610 eV, which is -0.746 eV less stable than O_{atop} site.

Table 1. Pd adsorption energy on each oxide surfaces.

Oxide / Adsorption site	Pd adsorption energy (eV)
ZrO ₂ / Obridge2	-2.012
ZrO ₂ / Obridge1	-2.287
ZrO ₂ / O _{atop}	-2.356
ZrO ₂ / Zr _{atop}	-1.610
MgO / O _{atop}	-1.511
MgO / Mg _{atop}	-0.738
CeO ₂ / Obridge2	-2.014
CeO ₂ / Obridge1	-2.038
CeO ₂ / O _{atop}	-1.846
CeO ₂ / Ce _{atop}	-0.786
CeO ₂ -DFT+U / Obridge2	-2.122
CeO ₂ -DFT+U / Obridge1	-2.003
CeO ₂ -DFT+U / O _{atop}	-1.819
CeO ₂ -DFT+U / Ce _{atop}	-0.707

Pd adsorption on MgO(100) surface is most favorable on O_{atop} site of surface oxygen atom. The adsorption energy of Pd on O_{atop} site is -2.24 eV. Adsorption on Mg_{atop} site results in a Pd atom positioned directly above surface oxygen atom and Pd adsorption energy on Mg_{atop} site is 0.773 eV less stable than the O_{atop} site.

In the case of CeO₂(110), Pd atom is most stable on Obridge1 site where Pd is positioned at the center between two surface oxygen atoms but different from Obridge2 site, and the calculated Pd adsorption energy is -2.038 eV, which is only 0.024 more stable than Obridge1 site. This result indicates that the stability of Pd adsorptions on Obridge2 and Obridge1 site is approximately equal. The most unstable Pd adsorption site is Ce_{atop} site where Pd is positioned directly above the surface Ce atom and the calculated Pd adsorption energy is -0.786 eV, which is -1.228 eV less stable than Obridge2 site. Mayernick and Janik also calculated Pd adsorption on CeO₂(110) surface, and they reported that the calculated Pd adsorption energies on Obridge2 and O_{atop} site are -1.78 and -1.68 eV, respectively [34], which are 0.23 and 0.21 eV lower than our calculated results, respectively, but showed similar site preference. We also calculated Pd adsorption on CeO₂(110) by DFT+U calculation. The most Pd adsorption site changes from Obridge2 to Obridge1 site, but energy difference is small (~0.12 eV). The other Pd adsorption site tendency is not affected by DFT+U method and Pd adsorption energy differences are within 0.1 eV between DFT and DFT+U.

Overall, the adsorption of atomic Pd on ZrO₂(110) is the most stable surface and O_{atop} site of ZrO₂(110) is the most favourable site for Pd atom. Obridge1 and Obridge2 sites of CeO₂(110) are the stable site next to ZrO₂(110) surface, whereas O_{atop} site of MgO(100) is the unstable surface. The most unstable Pd adsorptions on top of surface metal atoms are common characteristics in the three metal oxides, in particular CeO₂(110). Mayernick and Janik reported that the differences of Pd adsorption on CeO₂(111), (110), and (100) were due to interaction with surface oxygen atoms with coordination [34], and the surface formation energy of

CeO₂(100), 1.48 J/m² is much more endothermic than the (111) or (110) surfaces, 0.69 and 1.10 J/m², respectively [35]. From this, ZrO₂ is the same as CeO₂(110) and Pd adsorption energy difference between the most stable site of ZrO₂(110) and CeO₂(110) is small, about 0.3 eV.

Here, it is reported that the position of d-band center correlates with the catalytic activity and correlates changes in the energy center of the valence d-band state density of states at the surface sites with their ability to form chemisorption bond [36,37] as well as the adsorption of adsorbates [38]. Figure 2 shows the projected density of states (PDOS) of d electron of Pd atoms on ZrO₂(110) as examples. Pd adsorption energies are strong in order of O_{atop} (-2.356 eV), Obridge1 (-2.287 eV), and Obridge2 (-2.012 eV), and PDOS

of d electron on each adsorption site are shifted by that order, as shown in Figure 2. In addition, Figure 3 compares the adsorption energy of Pd on each metal oxide surfaces with those d electron density centers of Pd. In all cases, Pd adsorption energies on Obridge2, Obridge1, and O_{atop} site of each surfaces show linear correlation with the d electron density centers of Pd. Such linear correlations cannot be obtained when the d electron density centers of Pd adsorbed on surface metal atoms are included in this characteristic diagram. From this, it is considered that Pd on surface oxygen atom site and that on surface metal atom site are not the same but different properties. This result suggests that Pd adsorption on surface oxygen sites of metal oxide supports are controlled by d electron density centers of Pd.

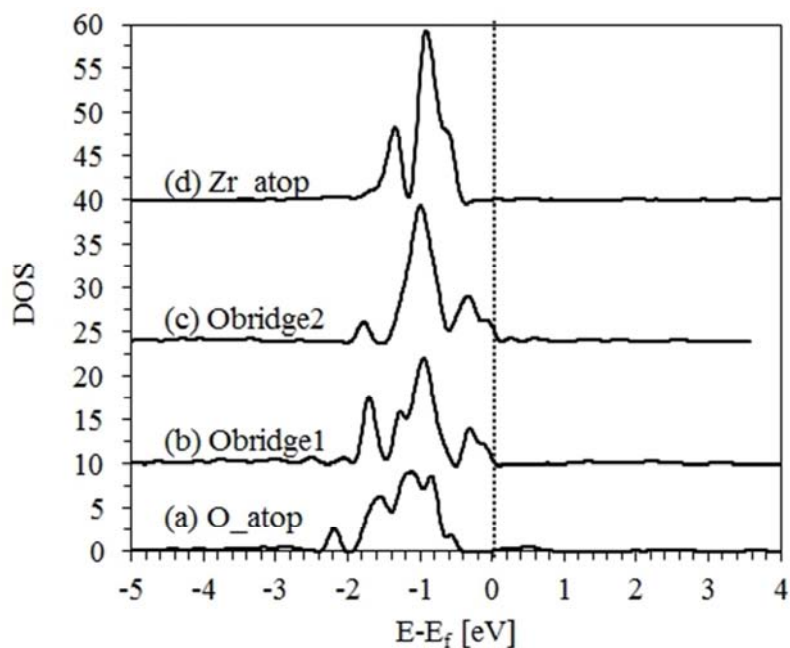


Figure 2. Projected density of states for d electron density of Pd adsorbed on (a) O_{atop}, (b) Obridge1, (c) Obridge2, and (d) Zr_{atop} sites of ZrO₂(110) surface. The Fermi level is set to 0 eV (dashed line).

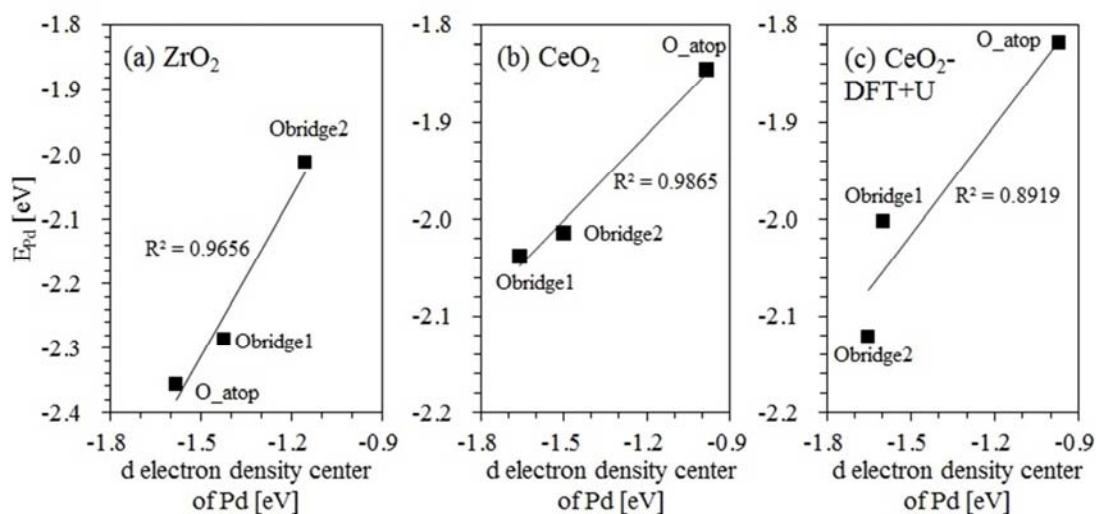


Figure 3. Pd adsorption energy (E_{Pd}) vs d electron density centers of Pd adsorbed on (a) ZrO₂(110), (b) CeO₂(110), and (c) CeO₂(110) calculated by DFT+U. The Fermi level is set to 0 eV.

3.2. CO Adsorption on Atomic Pd Supported on Oxide Surfaces

We calculated CO adsorption to evaluate how strong the CO adsorption on Pd on metal oxide surfaces is. In addition to metal oxide surfaces, we add a single Pd(111) crystal surface model for evaluation as a comparison object. Table 2 summarize the calculated adsorption energy of CO molecule on Pd atom adsorbed at the sites of single Pd(111) crystal surface, ZrO₂(110), MgO(100), CeO₂(110) surfaces, and CeO₂(110) surface calculated by DFT+U as shown in Figure 1. In the case of single Pd crystal surface, the most favorable site of CO molecule is determined to be hcp_hollow and fcc_hollow site where Pd is positioned at the center of three surface Pd atoms. The calculated CO adsorption energies on those sites are both -1.87 eV, while bridge and atop sites are 0.178 and 0.583 eV less stable than those sites, respectively. The calculated values of -1.87 eV are 0.33 ~ 0.44 eV lower than the experimental values (-1.54 [39] ~ -1.47 eV [40]), but 0.27 and 0.092 eV higher than the theoretical values (-2.14 eV (PW91) [41], 1.962 eV (PBE) [42]).

CO adsorption on Pd/ZrO₂(110) surface is the most favorable on Pd/ZrO₂(110)-Obridge2 site and the calculated CO adsorption energy is -2.273 eV. CO adsorption energy on Pd/ZrO₂(110)-O_atop site is -2.218 eV and only 0.055 eV different from that of Pd/ZrO₂(110)-Obridge2 site. The most unstable CO adsorption site of Pd/ZrO₂(110) is Zr_atop site (-1.342 eV) and Obridge1 site is next to (-1.646 eV), which is 0.931 eV and 0.627 eV less stable than the Obridge2 site, respectively.

Similarly, O_atop and Obridge2 sites of Pd/CeO₂(110) are the favorable for CO adsorption, which adsorption energies are -2.237 and -2.138 eV, respectively. The unstable CO adsorptions of Obridge1 and Ce_atop of Pd/CeO₂(110) are the same trend with Pd/ZrO₂(110). For Pd/CeO₂(110)

calculated by DFT+U, the site preference of CO is not changed.

From the above, atomic Pd on oxide surfaces shows about 0.4 eV stronger bonding to CO than Pd(111) crystal surfaces in this calculation. To understand the site preference of CO adsorption, we investigate the electronic structure of Pd atom adsorbed on oxide surfaces. Figure 4 shows the d electron density of CO adsorbed Pd surface atom in single Pd(111) crystal.

Table 2. CO adsorption energy on Pd atom and d electron density center of Pd adsorbed on single Pd(111) crystal surface, ZrO₂(110), MgO(100), CeO₂(110), and CeO₂(110) calculated by DFT+U oxide support surfaces. The Fermi level is set to 0 eV.

Support Material / Adsorption site	CO adsorption energy on Pd (eV)	d electron density centers of Pd (eV)
single Pd crystal / atop	-1.287	-3.096
single Pd crystal / bridge	-1.692	-2.467
single Pd crystal / fcc_hollow	-1.870	-2.258
single Pd crystal / hcp_hollow	-1.870	-2.261
ZrO ₂ / Obridge2	-2.273	-1.150
ZrO ₂ / Obridge1	-1.646	-1.421
ZrO ₂ / O_atop	-2.218	-1.581
ZrO ₂ / Zr_atop	-1.342	-1.052
MgO / O_atop	-2.244	-1.296
MgO / Mg_atop	-1.794	-0.270
CeO ₂ / Obridge2	-2.138	-1.498
CeO ₂ / Obridge1	-1.329	-1.658
CeO ₂ / O_atop	-2.237	-0.986
CeO ₂ / Ce_atop	-1.486	-1.007
CeO ₂ -DFT+U / Obridge2	-2.035	-1.650
CeO ₂ -DFT+U / Obridge1	-1.307	-1.599
CeO ₂ -DFT+U / O_atop	-2.255	-0.970
CeO ₂ -DFT+U / Ce_atop	-1.582	-0.864

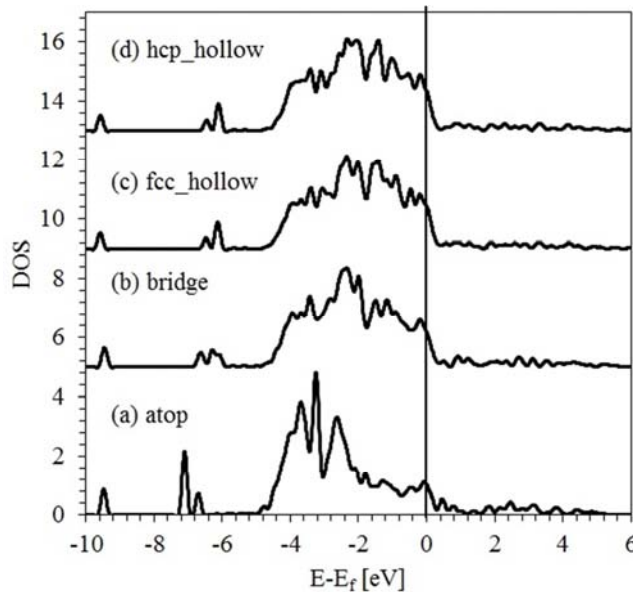


Figure 4. Projected density of states for d electron density of CO adsorbed Pd(111) surface atom for (a) atop, (b) bridge, (c) fcc_hollow, and (d) hcp_hollow sites. The Fermi level is set to 0 eV (solid line).

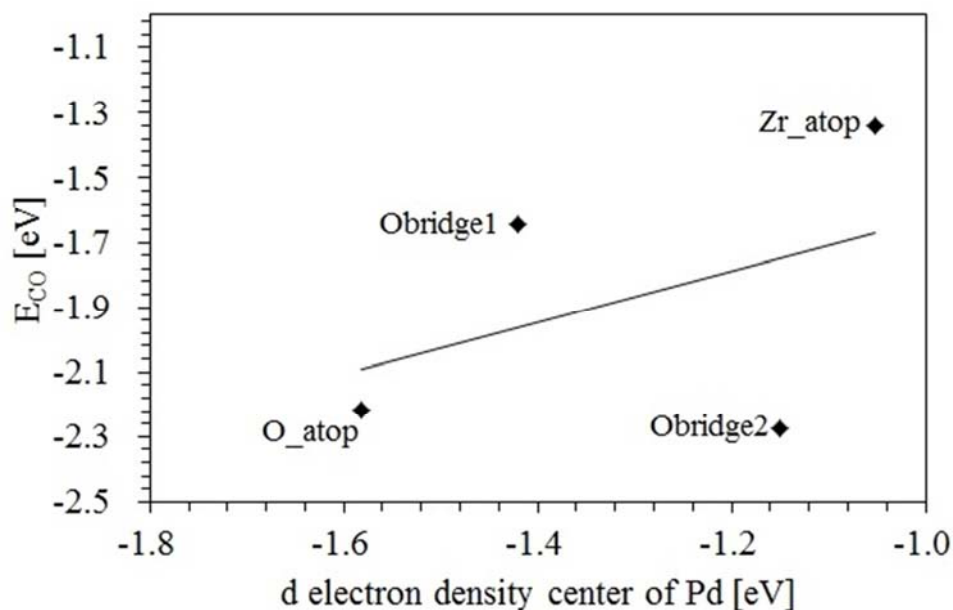


Figure 5. CO adsorption energy (E_{CO}) vs d electron density centers of Pd adsorbed on $ZrO_2(110)$. The Fermi level is set to 0 eV.

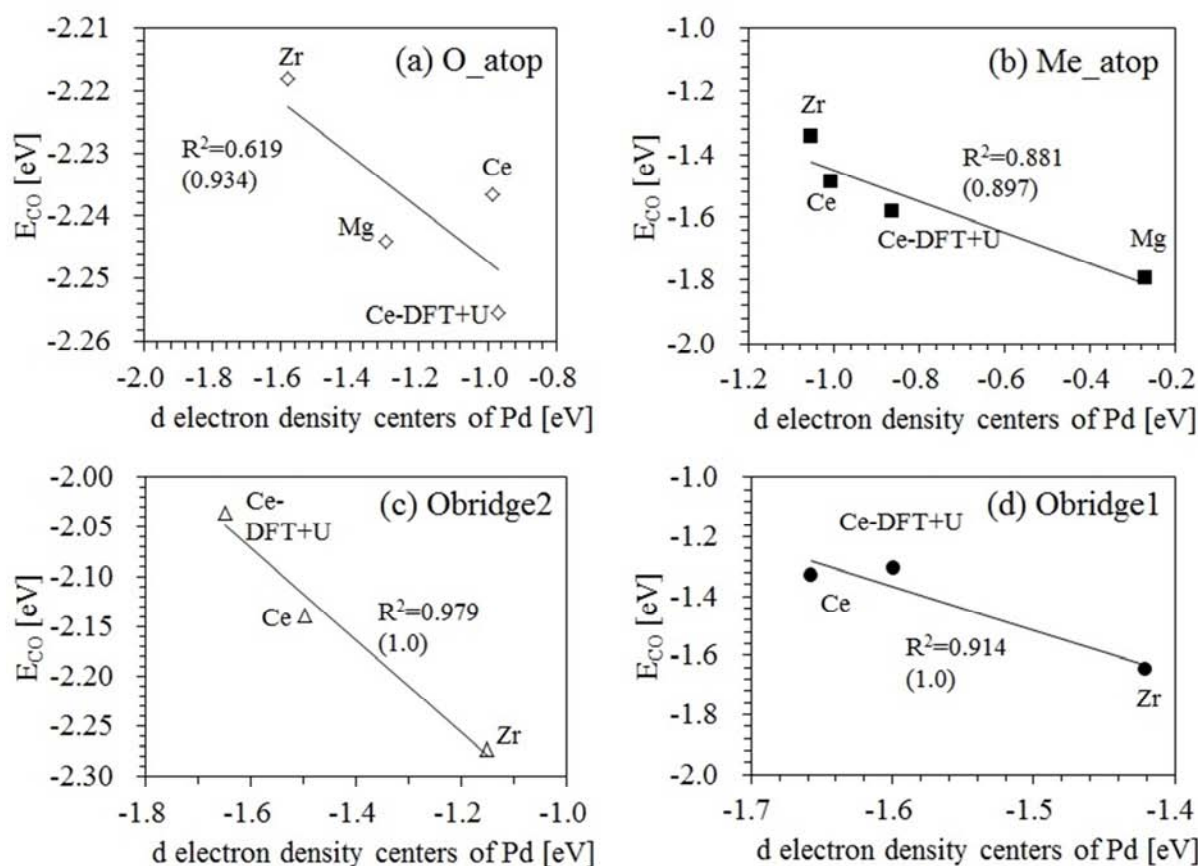


Figure 6. CO adsorption energy (E_{CO}) vs d electron density centers of Pd adsorbed on (a) O_atop , (b) Me_atop ($Me=Zr, Mg, Ce$), (c) $Obridge2$, and (d) $Obridge1$ sites of $ZrO_2(110)$, $MgO(100)$, $CeO_2(110)$, and $CeO_2(110)$ calculated by DFT+U. The values in parenthesis are R^2 values excluded $CeO_2(110)$. The Fermi level is set to 0 eV.

As shown in Figure 4, PDOS of d electron density of Pd are different from each adsorption site: the d electron density of Pd approaches the Fermi level as the CO adsorption energy increases. Here, it is reported that the position of d electron density center of Pd correlates with the catalytic

activity [36, 37] as well as the adsorption of adsorbates [38]. Since the CO adsorption energy on a simple Pd(111) surface shows the same tendency, the same can be said for the CO adsorption on Pd atom supported on oxide surface.

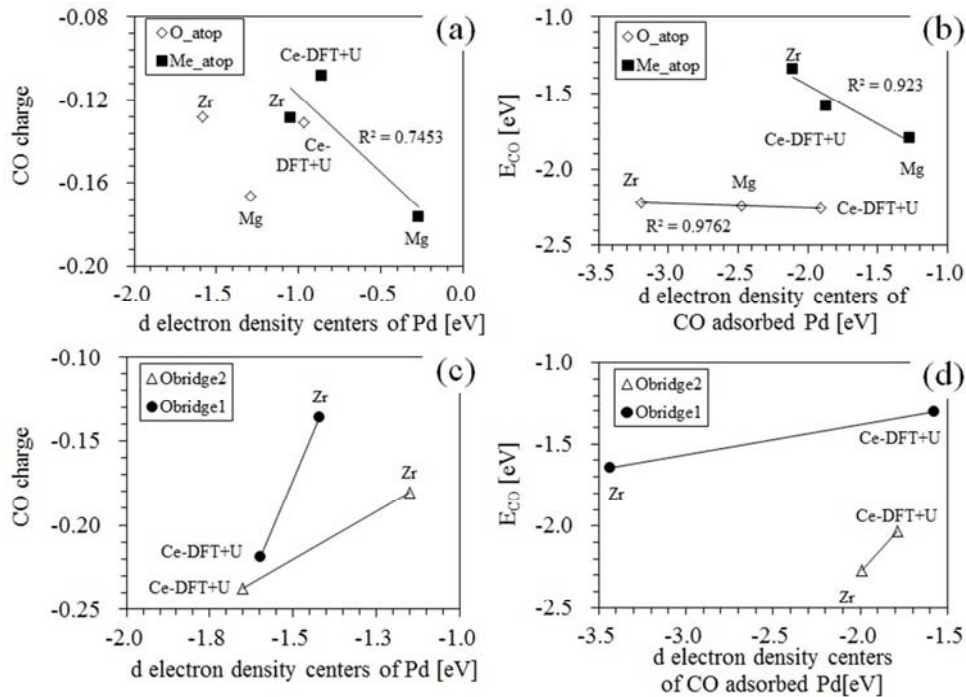


Figure 7. CO charge vs d electron density centers of Pd ((a) and (c)) adsorbed on O_{atop} , Me_{atop} ($Me=Zr, Mg, Ce$), $O_{bridge2}$, $O_{bridge1}$ sites, and CO adsorption energy (E_{CO}) vs d electron density centers of CO adsorbed Pd ((b) and (d)) adsorbed on ZrO₂(110), MgO(100), and CeO₂(110) calculated by DFT+U. The Fermi level is set to 0 eV.

Table 2 summarizes the d electron density centers of Pd adsorbed on the oxide surfaces, and Figure 5 shows the CO adsorption energy as a function of the d electron density center of Pd of Pd/ZrO₂(110) as an example. The CO adsorption energies on O_{atop} and $O_{bridge1}$ sites of Pd/ZrO₂(110) are almost the same (only 0.055 eV difference), but the d electron density center of Pd atoms showed different values. Therefore, in all three metal oxide surfaces, the d electron density center of Pd and CO adsorption energy do not correlate, even d electron density center of CO adsorbed Pd. As mentioned above, the result that the Pd adsorption energy on oxide surface is linearly related to the d electron density center of Pd except for surface metal atoms is obtained. Therefore, CO adsorption as well as Pd adsorption is considered to have different properties depending on adsorption sites. Figure 6 shows the relationship between CO adsorption energy and d electron density center of Pd for each adsorption site of Pd/ZrO₂(110), Pd/MgO(100), Pd/CeO₂(110).

At adsorption sites on oxide surfaces of the same material, the CO adsorption energy do not change with the position of the d electron density center of Pd. However, when divided by adsorption sites on Pd/oxide surfaces of different materials, CO adsorption energy increases as d electron density center of Pd approaches the Fermi level. As shown by the values in parentheses in Figure 6, it is better to calculate CeO₂(110) by DFT+U method due to now well-establishment difficulties within DFT to accurately represent the nature of 4f states in CeO₂ and that affects the adsorbates on CeO₂. From this result, it is possible to explain this result well by dividing how Pd adsorbs to the oxide surface even for

different materials. Since the CO adsorption energy and the position of the d electron density center of Pd are proportional, it is considered that the activity of Pd atom is controlled by the position of the d electron density center of Pd.

The close proximity of the d electron density center to the Fermi level means that it is easy to release electrons and it is difficult to receive. The d electron density center of Pd after CO adsorption is considered to be affected. As the d electron density center of Pd before CO adsorption approaches the Fermi level, that is, the electron donating property of Pd atom is higher, the CO charge is negatively larger as shown in Figure 7(a). From this, it is inferred that how to give electrons to CO or oxide surface determines the magnitude of CO adsorption energy for atop site Pd. Therefore, the larger the CO adsorption energy, the closer to the Fermi level the d electron density center of Pd after CO adsorption is, and Figure 7(b) represents this trend. On the contrary, The CO charge is negatively charged as the d electron density center of Pd on $O_{bridge2}$ and $O_{bridge1}$ site is far from the Fermi level, that is, the electron donating property of Pd is lower, as shown in Figure 7(c). When Pd adsorbs between two surface oxygen atoms, these bridged Pd atoms tend to stabilize by transferring electrons to another adsorbate or oxide surface since Pd electrons are insufficient. Therefore, it is considered that the CO adsorption energy is larger as the d electron density center of CO adsorbed Pd becomes farther from the Fermi level, and Figure 7 (d) shows this trend.

To confirm this concept, similar verification is carried out in a simple system such as atop type three atoms models of Me-O-Pd and O-M-Pd, bridge type 4 atoms model of

MeOO-Pd (see in Figure 1(e)). As shown in Figures 8(a) and 8(b), in the case of atop type models, the CO charge is negatively charged as the electron donating property of Pd is larger, and the closer the Fermi level the d electron density center of CO adsorbed Pd is, the higher the CO adsorption energy is. In the case of MeOO-Pd bridge type model, electron donating property of Pd does not correlate with CO charge as compared with atop type models. This trend is the same as for the oxide surface model. When separating with the same metal species, the CO adsorption energy is linearly proportional to the d electron density center of CO adsorbed Pd (Figures 8(c)-(e)), whereas it is not correlate in the case

of oxide surface model. Furthermore, CO adsorption energies in atop type models linearly correlate with the magnitude of CO charge in these simple models (as shown in Figure 9). Therefore, in these atomic models, correlation between CO adsorption and d electron density of Pd is clearly shown, especially atop type models (O-Me-Pd, Me-O-Pd). Oxide surface has more atoms and more complex structure than atomic models. The results of these simple systems suggest that Pd atom on the oxide surface are affected by surface atoms and adsorbed substances, and have different properties for each adsorption site since Pd atom is smallest size and susceptible to other atoms.

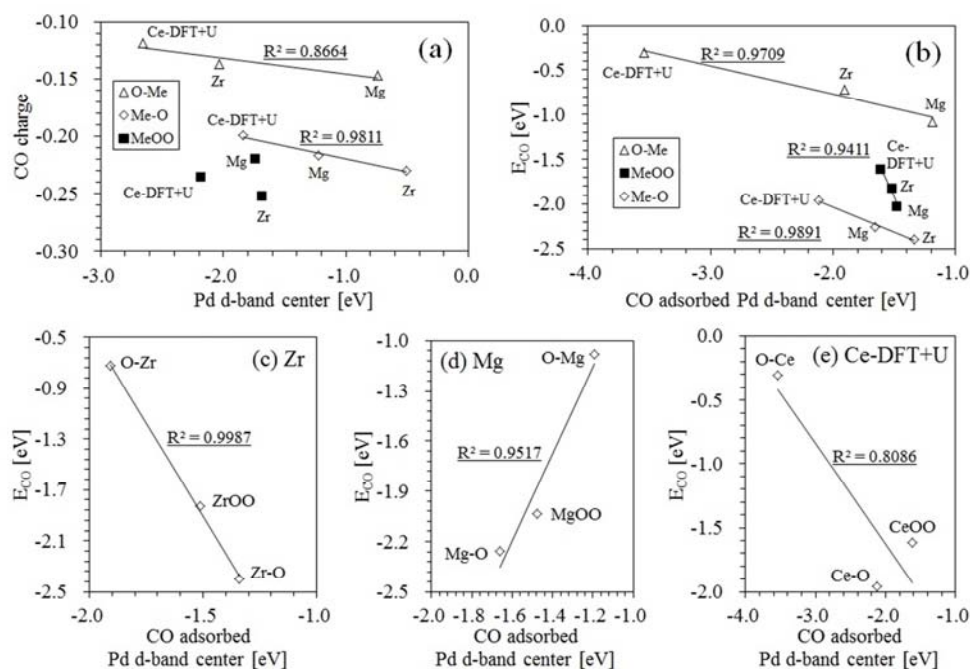


Figure 8. (a) CO charge vs d electron density center of Pd, and CO adsorption energy (E_{CO}) vs d electron density center of CO adsorbed Pd for (b) O-Me-Pd (Me=Zr, Mg, Ce) (white triangle), Me-O-Pd (white rhombus), MeOO-Pd (black square) molecules, and (c)-(e) same metal species. O-Me-Pd, Me-O-Pd, MeOO-Pd represent the Pd bonding to Me, O, two-oxygen bridge atoms, respectively. The Fermi level is set to 0 eV.

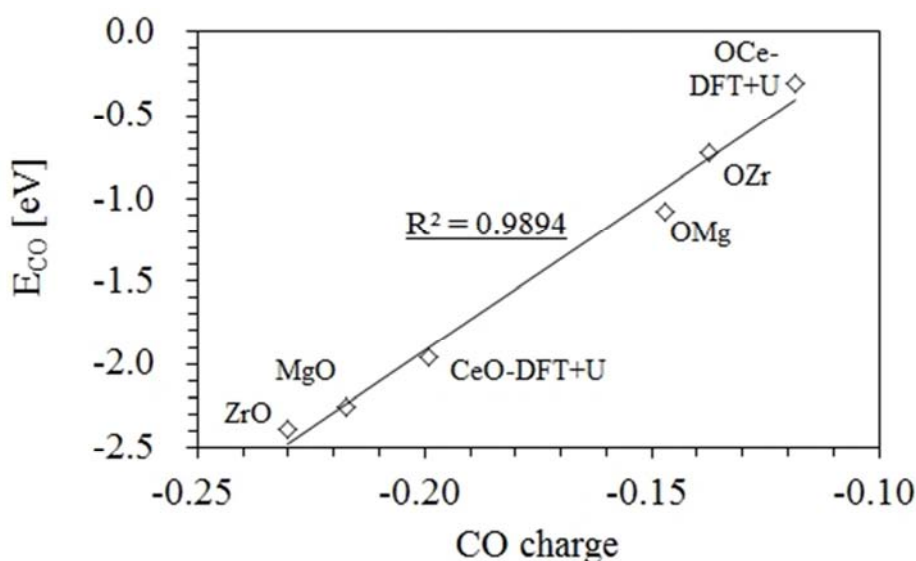


Figure 9. CO adsorption energy (E_{CO}) vs CO charge for Me-O-Pd (Me=Zr, Mg, Ce) and O-Me-Pd molecules. O-Me-Pd and Me-O-Pd represent the Pd bonding to Me and O atom, respectively.

4. Conclusion

In this study, we have performed DFT quantum periodic calculations to investigate the interaction between atomic Pd and oxide surfaces of ZrO₂(110), MgO(100), and CeO₂(110). As a calculated result of Pd adsorption to all sites of the three kinds of metal oxides, the most stable adsorption sites of ZrO₂, MgO and CeO₂ were O_{atop}, O_{atop} and Obridge 1, respectively. Conversely, the Me_{atop} site (on the surface metal atom) was the most unfavorable adsorption site in all oxide surfaces. From this, Pd tended to be more stable to bonds with surface oxygen atoms than surface metal atoms. It is well known that the position of the d-band center correlates with catalytic activity and adsorption [36-38]. In this study, we investigated the Pd adsorption energy supported on oxide surface and its relationship with d electron density center of Pd. On the surface of three kinds of oxides, the Pd adsorption energy linearly correlated with the position of d electron density center of Pd except for Pd on the surface metal atom sites. Therefore, it was inferred that Pd atoms have different properties depending on adsorption sites even on the same oxide surface.

Furthermore, the relationship between CO adsorption on Pd/oxide surface model and d electron density of Pd was investigated. In a simple system such as a single Pd(111) crystal surface, it is obvious that the d electron density center controls the activity of Pd for CO adsorption. In the case of oxide surface, the nature of Pd differs depending on whether Pd adsorbs on atop of the oxide surface atom or between two surface oxygen atoms. When Pd is adsorbed on atop of oxide surface atoms, the closer the d electron density center of Pd is to the Fermi level, that is, the higher the electron donating property of Pd, the more negative the CO charge is. Moreover, the closer the d electron density center of CO adsorbed Pd is to the Fermi level, the higher the CO adsorption energy is. On the other hand, When a Pd atom is adsorbed between two surface oxygen atoms, CO charge is negatively charged as the d electron density center of Pd is far from the Fermi level, that is, as the electron donating property of Pd is lower. Moreover, the CO adsorption energy increases as the d electron density center of CO adsorbed Pd becomes farther from the Fermi level. Therefore, the interaction between Pd and oxide surface differs depending on where Pd adsorbs, which affect the interaction between Pd atom and adsorbate (CO).

References

- [1] M. G. Burrows and W. H. Stockmayer, *Proc. R. Soc. London, Ser. A* 176, 474 (1940).
- [2] H. Kondoh, R. Tpyoshima, Y. Monya, M. Yoshida, K. Mase, K. Amemiya, and B. S. Man, *Catal. Today*, 260, 14 (2016).
- [3] H. C. Ham, J. A. Stephens, G. S. Hwang, J. Han, S. W. Nam, and Tae. H. Lim, *J. Phys. Chem. Lett.* 3, 566 (2012).
- [4] K. C. Taylor, *Catal. Rev.-Sci. Eng.* 35, 457 (1993).
- [5] A. Trovarelli, C. de Leitenburg, M. Boaro, and G. Dolvetti, *Catal. Today* 50, 353 (1999).
- [6] F. Gao, Y. L. Wang, and D. W. Goodman, *J. Am. Chem. Soc.* 131, 5734 (2009).
- [7] J. Y. Park, Y. Zhang, M. Grass, T. Zhang, and G. A. Somorjai, *Nano Lett.* 8, 673 (2008).
- [8] D. W. Yuan, Z. R. Liu, and J. H. Chen, *J. Chem. Phys.* 134, 054704/1 (2011).
- [9] M. Haruta, T. Kobayashi, H. Sano, and N. Yamada, *Chem. Lett.*, 16, 405 (1987).
- [10] M. Valden, X. Lai, and D. W. Goodman, *Science* 281, 1647 (1998).
- [11] A. Sanchez, S. Abbet, U. Heiz, W.-D. Schneider, H. Häkkinen, R. N. Barnett, and U. Landman, *J. Phys. Chem. A* 103, 9573 (1999).
- [12] B. Yoon, H. Häkkinen, U. Landman, A. S. Wörz, J.-M. Antonietti, S. Abbet, K. Judai, and U. Heiz, *Science* 307, 403 (2005).
- [13] M. S. Chen and D. W. Goodman, *Science* 306, 252 (2004).
- [14] H. An, S. Kwon, H. Ha, H. Y. Kim, and H. M. Lee, *J. Phys. Chem. C* 120, 9292 (2016).
- [15] A. A. Herzing, C. J. Kiely, A. F. Carley, P. Landon, and G. J. Hutchings, *Science* 321, 1331 (2008).
- [16] Z. Duan and G. Henkelman, *ACS Catal.* 5, 1589 (2015).
- [17] T. Takei, T. Akita, I. Nakamura, T. Fujitani, M. Okumura, K. Okazaki, J. Huang, T. Ishida, M. Haruta, *Adv. Catal.*, 55, 1 (2012).
- [18] A. Corma and P. Serna, *Science* 313, 332 (2006).
- [19] T. Hayashi, K. Tanaka, and M. Haruta, *J. Catal.* 178, 566 (1998).
- [20] B. Chowdhury, J. J. Bravo-Suárez, N. Mimura, Jiqing, K. K. Bando, S. Tsubota, and M. Haruta, *J. Phys. Chem. B* 110, 22995 (2006).
- [21] Q. Fu, H. Saltsburg, M. Flytzani-Stephanopoulos, *Science*, 301, 935 (2003).
- [22] M. Shekhar, J. Wang, W.-S. Lee, W. D. Williams, S. M. Kim, E. A. Stach, J. T. Miller, W. N. Delgass, and F. H. Ribeiro, *J. Am. Chem. Soc.* 134, 4700 (2012).
- [23] S. Yuan, L. Meng, and J. Wang, *J. Phys. Chem. C* 117, 14796 (2013).
- [24] H. S. Bengaard, J. K. Nørskov, J. Sehested, B. S. Clausen, L. P. Nielsen, A. M. Molenbroek, and J. R. Rostrup-Nielsen, *J. Catal.* 209, 365 (2002).
- [25] F. Abild-Pedersen, O. Lytken, J. Engbæk, G. Nielsen, I. Chorkendorff, and J. K. Nørskov, *Surf. Sci.* 590, 127 (2005).
- [26] A. Kokaji, N. Bonini, S. de Gironcoli, C. Sbraccia, G. Fratesi, and S. Baroni, *J. Am. Chem. Soc.* 128, 12448 (2006).
- [27] J. A. Dumesic, G. W. Huber, and M. Boundart, *Principles of Heterogeneous Catalysis* (Wiley-VCH, Weinheim, Germany, 2008).

- [28] P. Christopher, H. L. Xin, and S. Linic, *Nat. Chem.* 3, 467 (2011).
- [29] X. Y. Deng, B. K. Min, A. Guloy, and C. M. Friend, *J. Am. Chem. Soc.* 127, 9267, (2005).
- [30] Roald Hoffmann, SOLIDS and SURFACES, VCH Publishers (1988).
- [31] P. Giannozzi, S. Baroni, N. Bonini, M. Calandra, R. Car, C. Cavazzoni, D. Ceresoli, G. L. Chiarotti, M. Cococcioni, I. Dabo, A. Dal Corso, S. Fabris, G. Fratesi, S. de Gironcoli, R. Gebauer, U. Gerstmann, C. Gougoussis, A. Kokalj, M. Lazzeri, L. Martin-Samos, N. Marzari, F. Mauri, R. Mazzarello, S. Paolini, A. Pasquarello, L. Paulatto, C. Sbraccia, S. Scandolo, G. Sclauzero, A. P. Seitsonen, A. Smogunov, P. Umari, R. M. Wentzcovitch, *J. Phys.: Condens. Matter*, 21, 395502 (2009).
- [32] J. P. Perdew, J. A. Chevary, S. H. Vosko, K. A. Jackson, M. R. Pederson, D. J. Singh, and C. Fiolhais, *Phys. Rev. B* 46, 6671 (1992).
- [33] H. J. Monkhorst and J. D. Pack, *Phys. Rev. B* 13, 5188 (1976).
- [34] A. D. Mayernick and M. J. Janik, *J. Chem. Phys.* 131, 084701 (2009).
- [35] A. D. Mayernick and M. J. Janik, *J. Phys. Chem. C* 112, 14955 (2008).
- [36] B. Hammer and J. K. Nørskov, *Surf. Sci.* 343, 211 (1995).
- [37] B. Hammer, *Top. Catal.* 37, 3 (2006).
- [38] V. Pallassana and M. Neurock, *J. Catal.* 191, 301 (2000).
- [39] X. Guo and J. T. Yates, Jr., *J. Chem. Phys.* 90, 6761 (1989).
- [40] G. Ertl and J. Koch, *Z. Naturforsch.* 25a, 1906 (1970).
- [41] M. Gajdos, A. Eichler, and J. Hafner, *J. Phys.: Condens. Matter*, 16, 1141 (2004).
- [42] S. E. Mason, I. Grinberg, and A. M. Rappe, *Phys. Rev. B* 69, 161401 (R) (2004).